Jpn.J.Leprosy 76, 11-17(2007)

Moxifloxacin と garenoxacin の抗らい菌活性

儀同政一*
国立感染症研究所ハンセン病研究センター

〔受付：2006 年 10 月 20 日、掲載決定：2006 年 12 月 15 日〕

キーワード：Buddemeyer 法、garenoxacin(GRNX)、moxifloxacin(MFLX)、
ニューキノロン、ヌードマウス足蹠法

治療期間の短縮と薬剤耐性に対応するため、Buddemeyer 法とヌードマウス足蹠法を用いて、新規ニューキノロン系抗菌薬 moxifloxacin（MFLX；バイエル薬品）と garenoxacin（GRNX；富山化学工業）の抗らい菌活性を、rifampicin（RFP）、sparfloxacin（SPFX）、gatifloxacin（GFLX）、levofloxacin（LVFX）と比較検討した。

Buddemeyer 法での抗らい菌活性は、RFP ＞ MFLX ＞ SPFX ＞ GFLX ＞ GRNX, ≒ LVFX で、MFLX は SPFX より強い抗らい菌活性を示し、また GRNX は LVFX と同等の抗らい菌活性を示した。ヌードマウス足蹠法では MFLX の 10mg/kg でらい菌の増殖を完全に抑制し、SPFX より若干強い抗らい菌活性を示した。GRNX は 60mg/kg でらい菌の増殖を完全に抑制した。

はじめに

ハンセン病は、多剤併用療法の普及により有病率は低下したが、世界では今なお約 40 万人[1]の新患発生がみられ、治療面では PB で 6 ヵ月、MB で 1 年以上の長い期間を要し、耐性菌増加の問題も生じてきている。治療期間の短縮と薬剤耐性獲得に対応するめ rifampicin(RFP) を除き、らい菌に対する唯一殺菌作用を持つニューキノロン系薬は極めて重要である。既存ニューキノロン系薬の中で抗らい菌活性の最も強い sparfloxacin(SPFX)[2]は副作用として光線過敏症[3]がある。また 8－メトキシキノロンである gatifloxacin(GFLX)[4]は、光線過敏症[5]と非ステロイド性消炎鎮痛薬との相互作用などの副作用が少なく[6]抗らい菌活性は強いが、高血糖・低血糖[7,8]の発現がみられている。従って、抗らい菌活性が強く、かつ光線過敏症や薬物相互作用などの副作用の少ない新規ニューキノロン薬の開発が求められている。

moxifloxacin(MFLX)[9,10]は、キノロン骨格の 7 位にピロロピリジン基、8 位にメトキシ基を導入することで、強い抗菌力、薬物相互作用と光線過敏症などに対する安全性を重視してドイツ・バイエル社により開発された新規 8－メトキシキノロンである。MFLX の抗らい菌活性は、高用量短期併用療法[11,12]と単回併用療法[13]についての報告はあるが、単剤での同系統キノロン薬との抗らい菌活性を比較検討した報告はない。

また garenoxacin(GRNX)[14]は、従来のニューキノロン系薬の抗菌活性に必須とされたキノロン骨格の 6 位にフッ素基が無く、7 位にベンゾピロー

* Corresponding author:
国立感染症研究所ハンセン病研究センター
〒189-0002　東京都東村山市青葉町 4-2-1
TEL：042-391-8211　FAX：042-394-9092
E-mail：m-gidoh@nih.go.jp

ル基、8位にジフルオロメトキシ基を導入し既存ニューキノロン系薬とは異なった構造式を有する。MRSA や VRE などの薬剤耐性菌に対して強い抗菌活性を示し、光線過敏症や薬物相互作用などの副作用の少ない新規ニューキノロン系薬として富山化学と大正製薬で開発中の薬剤である。

今回筆者は、MFLX 及び GRNX と SPFX、GFLX、levofloxacin(LVFX) 及び RFP の *in vitro* 抗らい菌活性を Buddemeyer 法[15, 16]を用いて比較検討した。また MFLX と GRNX の単剤と SPFX の抗らい菌活性をヌードマウス足蹠法を用いて比較検討した。

材料と方法

1）らい菌：らい菌（Thai-53 株）を接種後 11 ヶ月目のヌードマウス（BALB/c）の後肢足蹠より集菌・精製[17]し、Shepard 法[18]により菌数計算後所定の濃度に希釈し Buddemeyer 法とヌードマウス足蹠法に用いた。

2）動物：ヌードマウス（BALB/c-*nu/nu*, 雌、5 週令）は、日本クレアから購入し、ビニールアイソレータ（三基科学工芸）の中で、滅菌したマウス用耐圧固形飼料（MB-6E、船橋農場）で飼育した。

3）抗菌薬：MFLX（バイエル薬品）、GRNX（富山化学工業）、SPFX（大日本住友製薬）、GFLX（杏林製薬）、LVFX（第一三共製薬）は各製薬会社から原末の提供を受けた。RFP（和光純薬）は市販品を用いた。

Buddemeyer 法に用いたニューキノロン系薬 (MFLX, GRNX, SPFX, GFLX, LVFX)は 0.2N-NaOH で、RFP は dimethyl sulfoxide で溶解後、pH7.0 の phosphate buffered saline(PBS) で最終濃度が 8.0、2.0、0.5、0.125 μg /ml になるように調整した。

ヌードマウス足蹠法に用いた抗菌薬は、実験 1 では、SPFX(10 mg/kg)、MFLX(1.0, 2.0, 5.0, 10 mg/kg)、実験 2 では、SPFX (10 mg/kg)、GRNX(40, 50, 60, 70 mg/kg) は 0.001%Tween80 含有 PBS(pH 7.0) で所定の濃度に調製後、－30℃で冷凍保存した。

4）抗らい菌活性の測定

（1）*in vitro* 法

Buddemeyer 法[15, 16]によった。即ち、4-ml のガラスバイアル中に 7H12 培地 500 μl、らい菌 ($1x10^7$) 100 μl、抗菌薬 300 μl（最終濃度：8、2.0、0.5、0.125 μg/ml）を加えよく混合する。このガラスバイアルのキャップを緩く締め、32℃の炭酸ガスふらん器で 4 日間培養後、^{14}C- パルミチン酸（56mCi/mmol, DuPont NEN）を 1 μCi 加え混合後、再びキャップを緩く締めたガラスバイアルを、NaOH- シンチレータで処理したろ紙片を入れた 18-ml ポリエチレンバイアルに入れキャップを強く締める。さらに 32℃のふらん器中で 7 日間培養を継続し、発生した $^{14}CO_2$ 量を液体シンチレーションカウンターで測定した。そして MFLX、GRNX と SPFX, GFLX, LVFX, RFP との抗らい菌活性を比較検討した。

（2）ヌードマウス足蹠法

ヌードマウスの両後肢足蹠に 1 足蹠当り 10^7 のらい菌を接種した。菌接種後 3 ヵ月から 5 ヵ月の 3 ヵ月間、ステンレスカテーテルで各抗菌薬を週 5 日、毎日経口投与した。菌接種後 8 ヵ月から 11 ヵ月まで、月 1 回、4 ヵ月間、1 群 2 匹、4 足蹠内のらい菌数を計測し、1 足蹠当りのらい菌数を求めた。

実験 1：MFLX(1.0, 2.0, 5.0, 10 mg/kg) と SPFX(10 mg/kg) との抗らい菌活性の比較検討。

実験 2：GRNX(40, 50, 60, 70 mg/kg) と SPFX(10 mg/kg) との抗らい菌活性の比較検討。

結　果

1）Buddemeyer 法での抗らい菌活性：8 ～ 0.125 μg/ml の全濃度域で RFP ＞ MFLX ＞ SPFX ＞ GFLX ＞ GRNX ≒ LVFX の順で、MFLX は SPFX より強い活性を示し、また GRNX は LVFX とほぼ同等の活性を示した（Table 1）。

2）ヌードマウス足蹠法：MFLX は 10 mg/kg の毎日 1 回、週 5 日の経口投与で菌接種 11 ヵ月後まで接種菌数以下で、マウス足蹠内のらい菌の増殖を完全に抑制し、SPFX より若干強い抗らい菌活性を示した（Fig. 1）。他方、GRNX は 60 mg/kg の毎日 1 回、週 5 日の経口投与で菌接種 11 カ月後まで接種菌数以下で、マウス足蹠内のらい菌の増殖を完全に抑制した（Fig. 2）。

考　察

ハンセン病の治療は、PBで6ヶ月、MBで1年に及ぶ長い期間に及ぶためDDSとRFPの両薬剤に対する耐性菌が増加しつつある。更に抗らい菌活性の弱いofloxacinの単剤または低用量の長期投与によるキノロン耐性も増加しつつある。従って、治療期間の短縮と菌の薬剤耐性獲得を防ぐため新規抗らい菌薬の開発が求められている。しかし、抗らい菌活性を示す抗菌薬は、DDS、B663、RFPとニューキノロン系のSPFX、GFLX、LVFX、OFLXなど、マクロライド系のclarithromycin、テトラサイクリン系のminocyclineに限られている。特に、らい菌に対して殺菌作用を有し、かつRFPに匹敵する強い抗らい菌活性を持つニューキノロン系薬は、ハンセン病の重要な抗菌治療薬である。

Table 1. *In vitro* anti-*M.leprae* activities of various new quinolones measured by Buddemeyer system

Drugs	μ g/ml	$\chi \pm \sigma$ (cpm)[a]	Inhibition(%) [b]
Control		50904 ± 477	
LVFX	8.0	21907 ± 651	57.0
	2.0	35071 ± 436	31.1
	0.5	40815 ± 861	19.8
	0.125	46725 ± 531	8.21
GRNX	8.0	23162 ± 730	54.5
	2.0	35013 ± 805	31.2
	0.5	41268 ± 1092	18.9
	0.125	45686 ± 480	10.3
GFLX	8.0	17148 ± 883	66.3
	2.0	26631 ± 555	47.7
	0.5	38889 ± 649	23.6
	0.125	44115 ± 809	13.3
SPFX	8.0	15482 ± 472	69.6
	2.0	21943 ± 599	56.9
	0.5	31577 ± 685	38.0
	0.125	43373 ± 613	14.8
MFLX	8.0	14266 ± 111	72.0
	2.0	20274 ± 372	60.2
	0.5	29737 ± 786	41.6
	0.125	40871 ± 162	19.7
RFP	8.0	13536 ± 351	73.4
	2.0	14735 ± 833	71.1
	0.5	20396 ± 260	59.9
	0.125	33930 ± 561	33.3

a. Data are given as the mean ± standard deviation of triplicate samples.

b. [(specimen of control group(c) - that of a drug group) /c]x 100 (%)

ところで、これまでのニューキノロン系薬の中で最も血中半減期が16.3時間（200 mg空腹時単回経口投与）と長く[19]、かつ最も強い*in vivo*抗らい菌活性を有するのはSPFX[2]であるが、光線過敏症惹起作用がある。光線過敏症を軽減するため開発された8－メトキシキノロンであるGFLX[4]は、血中半減期が7.1時間（200 mg空腹時単回経口投与用）と短く、かつ糖尿病患者の高血糖・低血糖の発現という副作用がある[7,8]。

今回筆者は、数種抗菌薬の抗らい菌活性を検討し、MFLXがBuddemeyer法とヌードマウス足蹠法によって、既存ニューキノロン系薬の中で最も強い活性を有するSPFX[2]と同等またはそれ以上の強い活性を有することを明らかにした。MFLXは優れた組織移行性、高い血中濃度と血中半減期

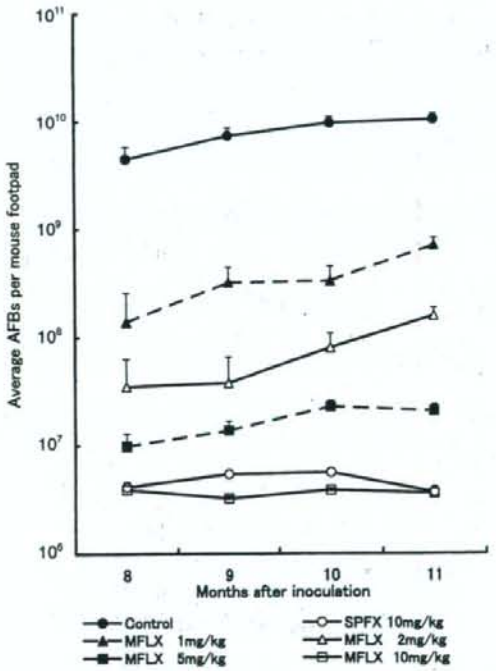

Fig. 1. Nude mice were infected with *M. leprae*, strain Thai-53, by inoculating $1x10^7$ bacilli into each of hind footpad, followed by oral administration of MFLX or SPFX, given once a day, 5 times weekly, between 3 to 5 months postinfection at a daily dose of 1.0, 2.0, 5.0 or 10 mg/kg. At 8, 9, 10 and 11 months after inoculation, mice were killed and the number of AFBs in the 4 hind footpads of 2 mice was counted according to the method of Shepard.

が 13.9 時間（400 mg 空腹時単回経口投与）[9] と長い新規８－メトキシキノロンで、400mg 、１日１回投与が可能である。

副作用としては、消化器系障害や肝機能検査値異常などが認められるが、発現率は LVFX と同程度であった[20]。MFLX は、光線過敏症や中枢神経系の副作用、非ステロイド性抗炎症薬やテオフィリンとの相互作用が低く[21]、耐性発現を抑制するなど優れた薬理学的特徴を持つ新規ニューキノロン系薬で、ハンセン病の治療に寄与すると考えられる。

GRNX[14] は、キノロン骨格の抗菌活性に必須とされていた６位にフッ素基が無く、既存ニューキノロン系薬と異なった構造式を持ち、Buddemeyer 法とヌードマウス足蹠法で LVFX とほぼ同等の抗らい菌活性を示した[22]。GRNX は、血中半減期が 12.6 時間（400 mg 空腹時単回経口投与）と長く、400mg 、１日１回投与が可能である。GRNX が MFLX と SPFX に比べ抗らい菌活性が弱かった原因として、蛋白結合率が約 87% で他のニューキノロンより高いこと、皮膚への移行性が劣ることなどが考えられる[23, 24]。

副作用としては、消化器系障害や肝機能障害などが認められるが発現率は低い[25]。

更に、GRNX は光線過敏症や中枢神経系への副作用、非ステロイド性抗炎症薬やテオフィリンとの相互作用などの副作用が極めて低く、特に関節毒性は現在本邦で唯一小児適用が認められている norfloxacin(NFLX) よりも弱い[26]。従って、小児から高齢者までのハンセン病患者に使用可能な新規ニューキノロン系薬となるであろうことが期待される。

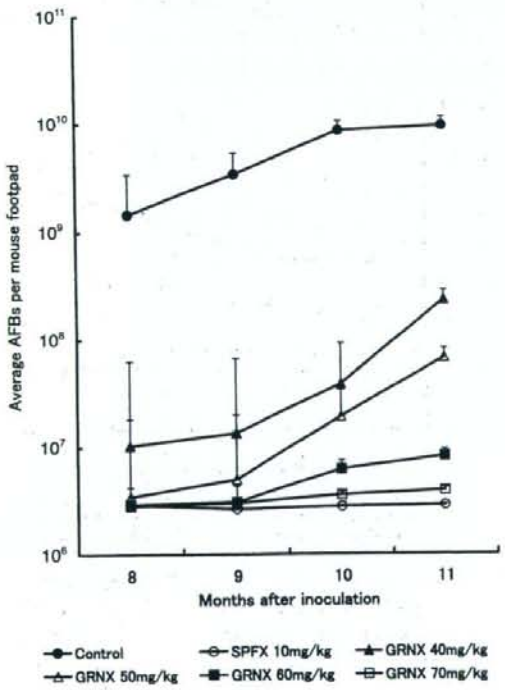

Fig. 2. Antibacterial activity of GRNX against *M. leprae* inoculated into footpads of nude mice. Inoculation of *M. leprae* and counting of AFBs were performed according to the methods as shown in the legend to Fig. 1.

本研究は、平成 17 年度厚生労働研究費補助金（新興・再興感染症研究事業）および平成 18 年度厚生労働研究費補助金（新興・再興感染症研究事業）の援助を受けた。

文　献

1）WHO Geneva. Weekly epidemiological record 80:289-296,2005.

2）Gidoh M ,Tsutsumi S : Activity of sparfloxacin against *Mycobacterium leprae* inoculated into footpads of nude mice. Lepr Rev 63:108-116,1992.

3）Michael E, Guido R, Fritz S, Ulrike H.: Defluorinated sparfloxacin as a new photoproduct identified by liquid chromatography coupled with UV detection and tandem mass spectrometry. Antimicrob Agents Chemother 42:1151-1159,1998.

4）Hosaka M, Yasue T, Fukuda H., Tomizawa H, Aoyama H, Hirai K : *In vitro* and *in vivo* antibacterial activities of AM-1155, a new 6-fluoro-8-methoxy quinolone. Antimicrob Agents Chemother 36: 2108-2117,1992.

5）草嶋久生、石田了三、内田　広：ニューキノロン系抗菌薬 Gatifloxacin および類薬のモルモットにおける光毒性．薬理と治療 26:1655-1660, 1998.

6) Nakashima M, Uematsu T, Kosuge K, Kusajima H, Ooie T, Masuda Y, Ishida R, Uchida H : Single- and multiple-dose pharmacokinetics of AM-1155, a new 6-fluolo-8-methoxy quinolone, in humans. Antimicrob Agents Chemother 39:2635-2640,1995.

7) Baker SE, Hangii MC : Possible gatifloxacininduced hypoglycemia. Ann Pharmacother 36:1722-1726,2002.

8) Biggs WS : Hypoglycemia and hyperglycemia associated with gatifloxacin use in elderly patients. J Am Board Fam Pract 16:455-457,2003.

9) Siefert HM, Domdey-Bette A, Henninger K, Kohlsdorfer C, Stass HH: Pharmacokinetics of the 8-methoxyquinolone, moxifloxacin : a comparison in humans and other mammalin species. J Antimicrob Chemother 43:69-76, 1999.

10) Dalhoff A, Petersen U, Endermann R : *In vitro* activity of BAY 12-8039, a new 8-methoxyquinolone. Chemotherapy 42:410-425,1996.

11) Consigny S, Bentoucha A, Bonnafous P, Grosset JJi B: Bactericidal activities of HMR-3647, moxifloxacin, and rifapentine against *Mycobacterium leprae* in mice. Antimicrob Agents Chemother 44:2919-2921 2000.

12) Baohong Ji, Perani EG, Petinom C, Grosset JH: Bactericidal activities of combinations of new drugs against *Mycobacterium leprae* in nude mice. Antimicrob Agents Chemother 40:393-399,1996.

13) Ji B Grosset J: Combination of rifapentine-moxiflxacin-minocycline(PMM) for the treatment of leprosy. Leprosy Rev 71: S81-87. 2000.

14) Takahata M, Mitsuyama J, Yamashiro Y, Yonezawa M, Araki H, Yodo Y, Minami S, Watanabe Y, Narita H: *In vitro* and *in vitro* antimicrobial activities of T-3811ME, a novel des-F(6)-quinolone. Antimicrob Agents Chemother 43:1077-1084, 1999.

15) Buddemeyer E, Hutchinson R, Cooper M : Automatic quantitative radiometric assay of bacterial metabolism. Clin Chem 22:1459 -1464,1976.

16) Franzblau SG : Oxidation of palmitic acid by *Mycobacterium leprae* in anaxenic medium. J Clin Microbiol 26:18-21,1988.

17) 中村昌弘：らい菌接種ヌードマウス足蹠乳剤内迷入雑菌の除去. 日ハンセン病会誌 64:47-50,1994.

18) Shepard CC, DH McRae: A method for counting acid-fast bacteria. Int J Lepr 36:78-82,1968.

19) 中島光好、金丸光隆、植松俊彦、滝口祥令：ピリドンカルボン酸系抗菌剤 Sparfloxacin の臨床第 I 相試験. 臨床医薬 7:1639-1684,1991.

20) 小林宏行、青木信樹、二木芳人、渡辺　彰、河合　伸、小田切繁樹、河野　茂、山口恵三、斉藤　厚：市中肺炎に対する levofloxacin を対照薬とした BAY 12-8039(moxifloxacin) 第Ⅲ相二重盲検比較検査. 日本化学療法学会雑誌　53 S-3:27-46,2005.

21) Balfour J, Wiseman L R : Moxifloxacin. Drug 57:363-373,1999.

22) 儀同政一：LVFX, ROM の抗らい菌活性. 日ハンセン病会誌 70: 78, 2001.

23) Andersson MI, MacGowan AP: Development of the quinolones. Antimicrob Agents Chemother 51:1-11,2003.

24) Hayakawa H, Fukushima Y, Kato H, Fukumoto H, Kadota H, Yamamoto H, Kuroiwa H, Nishigaki J, Tsuji A: Metabolism and disposition of novel des-fluoroquinolone garenoxacin in experimental animals and an interspecies scaling of pharmacokinetic parameters. Drug Metab Dispos 31: 1409 - 1418 ,2003.

25) Tellier G, Sullivan J, Fogarty C, Giordano P, Waskin H: Double-blind, randomized 5-day garenoxacin vs 7-to 10-day clarithromycin to treat community-acquired pneumonia. 45th ICAAC. 2005.

26) Nagai A, Miyazaki M, Morita T, Furubo S, Kizawa K, Fukumoto H, Sanzen T, Hayakawa H, Kawamura Y: Comparative articular toxic-

ity of garenoxacin, a novel quinolone antimicrobial agent, in juvenile beagle dogs. J Toxicol Sci 27:219-228,2002.

Jpn.J.Leprosy 76, 11-17(2007)

In vitro and *in vivo* activities of moxifloxacin and garenoxacin against *Mycobacterium leprae*

Masaichi GIDOH*
Leprosy Research Center, National Institute of Infectious Diseases

[Received: 20 Oct, 2006 / Accepted: 15 Dec, 2006]

Key words : Buddemeyer system, garenoxacin(GRNX), moxifloxacin(MFLX), new quinolones, nude mouse footpad method,

Moxifloxacin(MFLX) and garenoxacin(GRNX), new synthetic antibacterial agents, were assessed for *in vitro* anti-*M. leprae* activities. The anti-bacterial activities of these two drugs were compared to those of sparfloxacin (SPFX), gatifloxacin(GFLX), levofloxacin(LVFX) and rifampicin (RFP). The anti-*M. leprae* activity obtained by Buddemeyer system was stronger in order of RFP, MFLX, SPFX, GFLX and GRNX and LVFX.

The anti-*M. leprae* activity of MFLX or GRNX was also examined by the nude mouse footpad method. MFLX completely inhibited the growth of *M. leprae* inoculated into nude mouse footpads, when given orally at a daily dose of 10 mg/kg , while GRNX completely inhibited at a daily dose of 60 mg/kg. Both *in vitro* and *in vivo* tests indicated that MFLX was equal or superior to SPFX, but GRNX was equipotent to LVFX, in terms of anti-*M. leprae* activities.

*Corresponding author :
Leprosy Research Center, National Institute of Infectious Diseases,
4-2-1, Aoba-cho, Higashimurayama-shi, 189-0002 Tokyo, Japan.
TEL : +81-42-391-8211 FAX :+81-42-394-9092
E-mail : m-gidoh@nih.go.jp

ELSEVIER

INSTITUT PASTEUR

Microbes and Infection 9 (2007) 70–77

www.elsevier.com/locate/micinf

Original article

Contribution of GM-CSF on the enhancement of the T cell-stimulating activity of macrophages

Masahiko Makino*, Yumi Maeda, Yasuo Fukutomi, Tetsu Mukai

Department of Microbiology, Leprosy Research Center, National Institute of Infectious Diseases, 4-2-1 Aobacho, Higashimurayama, Tokyo 189-0002, Japan

Received 9 November 2005; accepted 10 October 2006
Available online 11 December 2006

Abstract

Mycobacterium leprae is an intracellular parasitic organism that multiplies in macrophages (MØ). It inhibits the fusion of mycobacterial phagosome with lysosome and induces interleukin (IL)-10 production from macrophages. However, macrophages are heterogenous in various aspects. We examined macrophages that differentiated from monocytes using either recombinant (r) granulocyte-MØ colony-stimulating factor (GM-CSF) (these MØ are named as GM-MØ) or rMØ colony-stimulating factor (M-CSF) (cells named as M-MØ) in terms of the T cell-stimulating activity. Although both macrophages phagocytosed the mycobacteria equally, GM-MØ infected with *M. leprae* and subsequently treated with IFN-γ- and CD40 ligand (L) stimulated T cells to produce interferon-gamma (IFN-γ), but M-MØ lacked the ability to stimulate T cells. While M-MØ mounted a massive IL-10 production, GM-MØ did not produce the cytokine on infection with *M. leprae*. *M. leprae*-infected, IFN-γ- and CD40L-treated GM-MØ expressed a higher level of HLA-DR and CD86 Ags than those of M-MØ, and expressed one of the dominant antigenic molecules of *M. leprae*, Major Membrane Protein-II on their surface. These results indicate that GM-CSF, but not M-CSF, contributes to the up-regulation of the T cell-stimulating activity of *M. leprae*-infected macrophages.

Keywords: Macrophage; *M. leprae*; GM-CSF; IFN-γ

1. Introduction

Mycobacterium leprae (*M. leprae*), a causative agent of human leprosy, is a representative parasitic pathogen that induces skin lesions and chronic progressive peripheral nerve injury, leading to systemic deformity [1,2]. Leprosy represents a clinical spectrum, in which clinical manifestations are associated with different levels of immune responses to *M. leprae* infection [3]. One representative type is a tuberculoid leprosy, in which patients exhibit innate and adaptive immunities to *M. leprae* and manifest a localized form of the disease with granuloma formation in infected tissues [4–6]. For the activation of an adaptive immunity, dendritic cells (DC) derived from inflammatory monocytes, play a central role [7,8]; and, in *in vitro* experiments, both $CD4^+$ and $CD8^+$ T cells are activated by DC infected with *M. leprae*, and these DC expressed Major Membrane Protein-II (MMP-II) as a dominant antigenic molecule [9,10]. Another representative manifestation is lepromatous leprosy, in which patients show reduced levels of host defense associated immunities and manifest a disseminated form of the disease with a broad spread of foamy MØ, in which an abundance of bacilli are usually involved [11,12]. *M. leprae* resides in the phagosome in MØ and replicates there without being digested by lysosomal enzymes [13]. Furthermore, *M. leprae* stimulates MØ to produce IL-10 [5,6] and suppresses the DC-mediated Ag-specific

Abbreviations: Ag, antigen; APC, Ag-presenting cells; BCG, *Mycobacterium bovis* BCG; DC, dendritic cells; GFP-BCG, BCG expressing GFP; GM-CSF, granulocyte-macrophage colony-stimulating factor; IFN-γ, interferon-gamma; IL, interleukin; L, ligand; mAb, monoclonal antibody; MØ, macrophages; M-CSF, MØ colony-stimulating factor; *M. leprae*, *Mycobacterium leprae*; MMP-II, Major Membrane Protein-II; PBMC, peripheral blood mononuclear cells; r, recombinant.

* Corresponding author. Tel.: +81 42 391 8059; fax: +81 42 391 8212.
E-mail address: mmaki@nih.go.jp (M. Makino).

1286-4579/$ - see front matter © 2006 Elsevier Masson SAS. All rights reserved.
doi:10.1016/j.micinf.2006.10.011

adaptive immunity [14,15]. These observations may indicate that the induction of intracellular processing of *M. leprae* and that of expression of molecules, such as MMP-II could lead to the activation of IFN-γ producing type 1 $CD4^+$ T cells. Another important element that should be considered for the full activation of T cells is the suppression of IL-10 production from *M. leprae*-infected MØ.

So far, a variety of methods and tools, including cytokines, have been used for the differentiation of MØ from human peripheral monocytes *in vitro* [16–18]. One representative MØ can be differentiated by using M-CSF, termed M-MØ, and another by using GM-CSF, termed GM-MØ. Both MØ represent different functions on infection with mycobacteria. However, much remains not fully understood with regard to *M. leprae* infection and the T cell-stimulating activity of these MØ.

In this report, we analyzed the characteristics of *M. leprae*-infected GM-MØ and M-MØ, and tried to develop immunological methods to enhance the MØ-mediated host defense activities against the bacteria.

2. Materials and methods

2.1. Preparation of cells and bacteria

Peripheral blood was obtained from healthy PPD-positive individuals under informed consent. We are aware that PPD-negative individuals would help to provide more information for our study; however, in Japan, most healthy individuals are PPD-positive, because *Mycobacterium bovis* BCG vaccination is compulsory for children (0–4 years old). Moreover, PPD-negative individuals in the Japanese population are those who do not respond to BCG vaccination, and therefore, it is likely that they suffer from some immune insufficiency. Therefore, these individuals cannot be used as controls for our experiments. Peripheral blood mononuclear cells (PBMC) were isolated using Ficoll-Paque Plus (Pharmacia, Uppsala, Sweden) and cryopreserved in liquid nitrogen until use, as previously described [19]. For preparation of peripheral monocytes, $CD3^+$ T cells were removed from either freshly isolated heparinized blood, or cryopreserved PBMC using immunomagnetic beads coated with anti-CD3 monoclonal antibody (mAb) (Dynabeads 450, Dynal, Oslo, Norway). The $CD3^-$ PBMC fraction was plated on collagen-coated plates and the non-plastic adherent cells were removed by extensive washing. The remaining adherent cells were used as monocytes [19]. MØ were differentiated by culturing monocytes in the presence of 20% fetal calf serum and either rM-CSF (R and D Systems, Abingdon, UK) (M-MØ) or rGM-CSF (Pepro Tech EC LTD, London, UK) (GM-MØ) [20]. Both GM-MØ and M-MØ were pulsed with *M. leprae*, treated with an optimal dose of IFN-γ on day 3 of culture, further treated with CD40L on day 4, and were used as a stimulator of T cells on day 5 [21]. *M. leprae* (Thai-53) was isolated from the footpads of BALB/c-*nu/nu* mice [22]. The isolated bacteria were counted by Shepard's method [22]. Killed *M. leprae* was prepared by heating the bacteria at 60 °C for 18 h. BCG (Pasteur strain) was cultured *in vitro* using Middlebrook 7H9 broth supplemented with 0.05% Tween 80 and albumin-dextrose-catalase. BCG expressing GFP was constructed as follows. The GFP sequence was amplified from pEGFP-1 vector (CLONTECH, Palo Alto, CA), and cloned into pMV261 [23]. Transformants were selected on a 7H10 plate containing 25 μg/ml kanamycin. The phagocytosis of BCG by GM-MØ and M-MØ after culture was determined using FACScalibur (Becton Dickinson Immunocytometry System, San Jose, CA). The multiplicity of infection (MOI) was determined based on the assumption that MØ were equally susceptible to infection with *M. leprae* [24].

2.2. Analysis of cell surface antigen (Ag)

The expression of cell surface Ag on MØ was analyzed using FACScalibur. Dead cells were eliminated from the analysis by staining with propidium iodide (Sigma Chemical Co., St. Louis, MO) and 1×10^4 live cells were analyzed. For analysis of cell surface Ag, the following mAbs were used: FITC-conjugated mAb against HLA-ABC (G46-2.6, PharMingen, San Diego, CA), HLA-DR (L243, PharMingen), CD14 (M5E2, BD Biosciences, San Jose, CA), TLR2 (TL2.3, Serotec, Oxford, UK), TLR4 (HTA125, Santa Cruz Biotech, Santa Cruz, CA), CD209 (DCN46, PharMingen), CD86 (FUN-1, PharMingen), and CD40 (5C3, PharMingen).

The expression of MMP-II, which is one of the dominant antigenic molecules of *M. leprae* [9] on *M. leprae*-infected MØ was determined using the mAb (IgM, kappa) against MMP-II, followed by FITC-conjugated anti-mouse Igs Ab (Tago-immunologicals, Camarillo, CA).

2.3. APC function of M. leprae-infected MØ

The ability of *M. leprae*-infected MØ to stimulate T cells was assessed using an autologous MØ-T cell co-culture as previously described [24,25]. Freshly thawed PBMC were depleted of $CD56^+$, MHC class II^+ and $CD8^+$ cells by using magnetic beads coated with mAb to CD56, MHC class II and CD8 Ags (Dynabeads 450; Dynal) [25]. The purity of $CD4^+$ T cells was more than 98% as assessed by FACS analyses. The purified responder cells (1×10^5 per well) were plated in 96-well round-bottom tissue culture plates and MØ were added to give the indicated MØ:$CD4^+$ T cell ratio. Supernatants of MØ-T cell co-cultures were collected on day 4 and the concentration of cytokines was determined.

2.4. Cytokine production

Levels of the following cytokines were measured; IFN-γ produced by $CD4^+$ T cells, IL-10, IL-1β, TNFα and IL-12p40 produced by MØ stimulated for 24 h with *M. leprae*. The concentrations of these cytokines were quantified using the enzyme assay kits, Opt EIA Human ELISA Set (BD PharMingen International).

2.5. Statistical analysis

Student's *t*-test was applied to determine the statistical differences.

3. Results

3.1. Characteristics of MØ differentiated from monocytes using GM-CSF

MØ were differentiated from monocytes using either GM-CSF (GM-MØ) or M-CSF (M-MØ). To characterize these two types of MØ, surface markers expressed on GM-MØ and M-MØ were analyzed using the monocytes obtained from the same donor by flow cytometry (Fig. 1). MHC class I (HLA-ABC) and class II (HLA-DR) Ags were similarly expressed on GM-MØ and M-MØ, but the expression of CD14 Ag was significantly reduced in GM-MØ. While the expression level of TLR2, CD209, CD40 and TLR4 Ags was not different between GM-MØ and M-MØ, the expression of CD86 was significantly higher on GM-MØ than M-MØ. Then, we examined the phagocytic capacity of GM-MØ and M-MØ by using BCG expressing GFP (GFP-BCG), since *M. leprae* cannot be cultured *in vitro* or express GFP. The percentage of MØ expressing GFP after co-culture of MØ with GFP-BCG was similar between GM-MØ and M-MØ (Fig. 2). These results indicate that GM-MØ and M-MØ differed in the expression of some surface markers, but they similarly phagocytosed the mycobacteria.

3.2. Effect of M. leprae infection to GM-MØ on the T cell-stimulating activity

Since *M. leprae* is an intracellular parasitic bacterium and is hardly digested with lysosomal enzyme in MØ unless MØ are activated [26], we analyzed the T cell-stimulating activity of *M. leprae*-infected GM-MØ and M-MØ (Table 1). When M-MØ were infected with up to MOI 80 of *M. leprae* and treated with IFN-γ and CD40L, they did not stimulate $CD4^+$ T cells to secrete a significant dose of IFN-γ. In contrast to M-MØ, when *M. leprae*-infected, IFN-γ- and CD40L-treated GM-MØ were used as Ag-presenting cells (APC), T cells produced significant levels of IFN-γ in a manner dependent on the dose of *M. leprae*. Since GM-MØ express CD40, and are activated by IFN-γ, we examined the effect of treatment with IFN-γ and CD40L on the T cell-stimulating activity of *M. leprae*-infected GM-MØ (Table 2). While IFN-γ production from $CD4^+$ T cells was not significantly induced by GM-MØ untreated or treated with either IFN-γ or CD40L, the cytokine production was significantly enhanced by the treatment of GM-MØ with

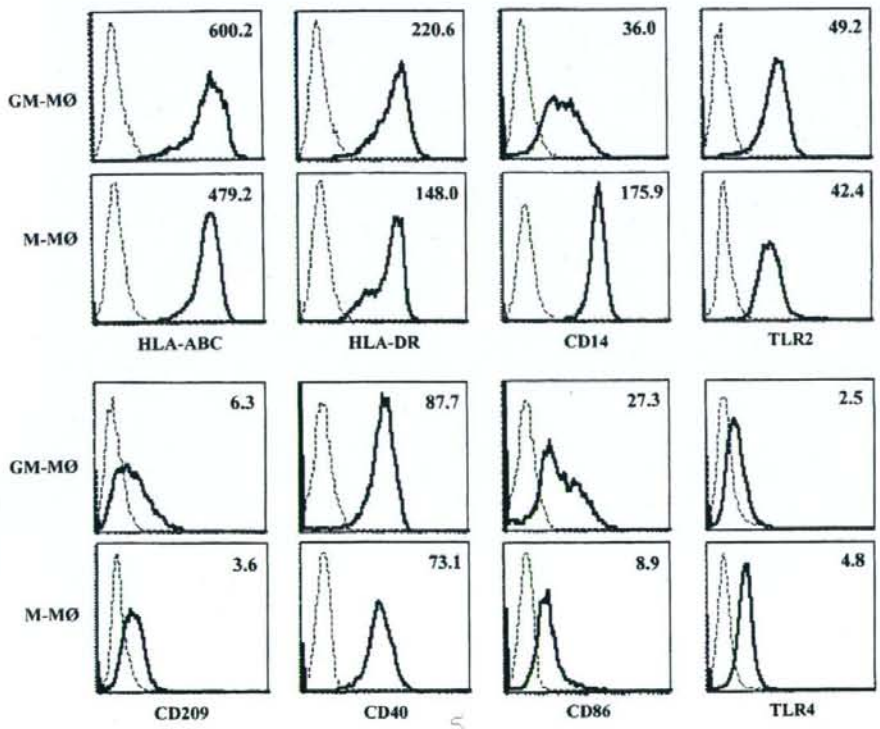

Fig. 1. Phenotype of GM-MØ and M-MØ differentiated from monocytes. Plastic adherent monocytes were differentiated into MØ by 3 days culture with either rGM-CSF or rM-CSF. Dashed lines, isotype-matched control IgG; solid lines, mAb staining. The number represents the difference in mean fluorescence intensity between dashed and solid lines. Representatives of three independent experiments are shown.

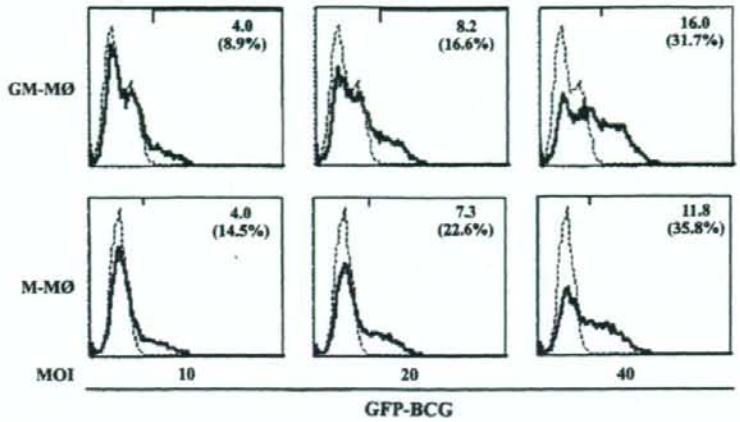

Fig. 2. Phagocytic activity of GM-MØ and M-MØ. Plastic adherent monocytes were differentiated into MØ by 3 days culture with either rGM-CSF or rM-CSF. For analysis of the phagocytic activity of MØ, GM-MØ and M-MØ were pulsed with BCG expressing GFP and assessed on day 4 of culture. Dashed lines, unpulsed cells; solid lines, GFP-BCG pulsed cells. The number represents the difference in mean fluorescence intensity between the dashed and solid lines. The number in parenthesis indicates the percent GFP-positive cell number. Representatives of three independent experiments are shown.

both IFN-γ and CD40L. Then, we compared the T cell-stimulating activity of live and heat-killed *M. leprae* (Table 3). Both forms of *M. leprae* stimulated $CD4^+$ T cells when pulsed to GM-MØ, but the heat-killed *M. leprae* more efficiently induced T cell activation than live bacteria. When we examined the effect of heat-killed *M. leprae* on M-MØ, they did not stimulate $CD4^+$ T cells significantly, even when IFN-γ and CD40L were administered (data not shown). Also note that, when GM-MØ and monocyte-derived DC were compared in terms of their T cell-stimulating activity, GM-MØ were less efficient in this respect (data not shown).

3.3. Factors associated with the enhancement of the T cell-stimulating activity of GM-MØ

Various factors may be responsible for enhancing the T cell-stimulating activity of APC. When we examined the expression of APC associated molecules on *M. leprae*-infected MØ (Fig. 3), the expression of HLA-DR and CD86 on GM-MØ was higher than on M-MØ, although there was no significant difference in the expression of HLA-ABC between GM-MØ and M-MØ. The cytokines produced from APC should also be considered to be another important factor that should be monitored and MØ produce a variety of cytokines, including IL-10, IL-1β, TNFα and IL-12 [6,11,27]. IL-10 was efficiently produced from M-MØ by stimulation with *M. leprae*, but it was hardly produced from GM-MØ (Fig. 4a). When macrophages were differentiated by using both GM-CSF and M-CSF, the function of GM-CSF was dominant and, the production of IL-10 was suppressed (Fig. 4a). Similarly to the production of IL-10, IL-1β was more efficiently produced from M-MØ than GM-MØ (Fig. 4b). In contrast, TNFα, which is important for granuloma formation, was more efficiently produced from GM-MØ (Fig. 4c). However, there was no significant difference in the production of IL-12p40 between GM-MØ and M-MØ (Fig. 4d). Finally, we assessed whether *M. leprae*-infected GM-MØ expressed dominant antigenic molecules of *M. leprae* on the surface (Fig. 5). To this end, we examined the expression of MMP-II on GM-MØ and M-MØ. No apparent expression of

Table 1
T cell-stimulating activity of *M. leprae*-infected GM-MØ and M-MØ[a]

Stimulator of $CD4^+$ T cells	*M. leprae* infection of macrophages (MOI)	IFN-γ (pg/ml) production by $CD4^+$ T cells after stimulation with macrophages at ratio (T:MØ)		
		2:1	4:1	8:1
GM-MØ	0	$0.6 \pm 0.2^{*,\dagger}$	$0.5 \pm 0.1^{\ddagger,\S}$	$1.4 \pm 0.2^{\P,\|}$
	40	$38.1 \pm 3.8^{*}$	$34.2 \pm 2.3^{\ddagger}$	$23.4 \pm 3.8^{\P}$
	80	$230.7 \pm 21.4^{\dagger}$	$120.5 \pm 16.9^{\S}$	$74.7 \pm 6.8^{\|}$
M-MØ	0	0.9 ± 0.1	3.1 ± 1.2	13.9 ± 2.2
	40	0.9 ± 0.1	2.6 ± 1.3	12.2 ± 3.1
	80	11.8 ± 0.3	17.5 ± 2.1	12.2 ± 2.9

$^{*}p < 0.005$; $^{\dagger}p < 0.005$; $^{\ddagger}p < 0.01$; $^{\S}p < 0.01$; $^{\P}p < 0.01$; $^{\|}p < 0.005$.

[a] $CD4^+$ T cells (1×10^5/well) were stimulated for 4 days with autologous GM-MØ or M-MØ at the indicated dose of macrophage. GM-MØ or M-MØ were pulsed with *M. leprae* and IFN-γ (100 IU/ml) on day 3, treated with CD40L (1 μg/ml) on day 4, and were used as APC on day 5. Representatives of three separate experiments are shown. Assays were done in triplicate, and results are expressed as mean ± SD. Groups with identical symbols were compared using Student's *t*-test.

Table 2
Contribution of IFN-γ and CD40L on T cell-stimulating activity of GM-MØ[a]

M. Leprae infection of GM-MØ (MOI: 80)	Treatment of *M. leprae*-infected GM-MØ with		IFN-γ (pg/ml) production by $CD4^+$ T cells after stimulation with GM-MØ at ratio (T:MØ)		
	IFN-γ (100 IU/ml)	CD40L (1.0 μg/ml)	2:1	4:1	8:1
−	+	+	2.3 ± 0.3	0.1 ± 0.2	0.8 ± 0.5
+	−	−	$4.0 \pm 1.1^{*}$	$5.5 \pm 1.9^{\S}$	$6.0 \pm 2.1^{\#}$
+	−	+	$21.4 \pm 3.1^{\dagger}$	$22.7 \pm 4.0^{\P}$	$14.8 \pm 2.2^{**}$
+	+	−	$20.3 \pm 1.7^{\ddagger}$	$15.9 \pm 1.3^{\|}$	$10.7 \pm 2.3^{\dagger\dagger}$
+	+	+	$226.1 \pm 20.9^{*,\dagger,\ddagger}$	$107.8 \pm 13.7^{\S,\P,\|}$	$94.8 \pm 9.7^{\#,**,\dagger\dagger}$

$^{*}p < 0.005$; $^{\dagger}p < 0.005$; $^{\ddagger}p < 0.005$; $^{\S}p < 0.005$; $^{\P}p < 0.005$; $^{\|}p < 0.01$; $^{\#}p < 0.005$; $^{**}p < 0.005$; $^{\dagger\dagger}p < 0.005$.

[a] $CD4^+$ T cells (1×10^5/well) were stimulated for 4 days with autologous GM-MØ at the indicated dose of macrophage. GM-MØ were pulsed with *M. leprae* and IFN-γ (100 IU/ml) on day 3, treated with CD40L (1 μg/ml) on day 4, and were used as APC on day 5. Representatives of three separate experiments are shown. Assays were done in triplicate, and the results are expressed as the mean ± SD. Groups with identical symbols were compared using Student's *t*-test.

MMP-II was observed on M-MØ, but, on GM-MØ, significant expression of MMP-II was induced. The expression was dependent on the dose of *M. leprae* (Fig. 5). However, the MMP-II expression on *M. leprae*-infected GM-MØ required both IFN-γ and CD40L, and apparent expression was not induced by sole treatment of macrophages with either IFN-γ or CD40L (data not shown).

4. Discussion

In order to avoid the intracellular multiplication and intercellular spread of *M. leprae*, the activation of adaptive immunity, especially of IFN-γ-producing type 1 T cells, plays an important role [5,6]. In fact, paucibacillary (tuberculoid) leprosy patients activate $CD4^+$ T cells through DC, although the bacteria cannot be eliminated completely [8,28]. The *M. leprae*-infected DC digest the bacteria and express dominant antigenic molecules for the efficient IFN-γ production from T cells [9]. In contrast, multibacillary (lepromatous) leprosy patients retain a large number of *M. leprae* in their MØ, and concordantly induce reduced levels or completely lack the ability to effectively stimulate T cells [11,12]. Since tissue resident MØ are heterogenous with regard to functional aspects [17,29], we assessed two different types of MØ: GM-MØ and M-MØ, and found that GM-MØ, but not M-MØ, stimulated T cells. GM-MØ were generated from monocytes using cytokine GM-CSF whilst M-MØ were produced using M-CSF. Although there were some differences in the expression levels of MHC class I, II, CD14 and CD209 Ags on GM-MØ and M-MØ, both forms were equally susceptible to mycobacteria as far as phagocytosis of BCG-GFP was examined. However, there was a striking difference between *M. leprae*-infected GM-MØ and M-MØ in the expression of antigenic molecules; only GM-MØ expressed MMP-II, which is one of the dominant antigenic molecules capable of stimulating T cells in *M. leprae*-infected individuals. The induction of MMP-II expression on GM-MØ requires not only GM-CSF, but also the co-stimulation of MØ with IFN-γ and CD40L. In case of *M. leprae*-infected DC, the phagosomal bacteria could be processed by lysosomal enzymes, and MMP-II expression was observed on DC [9]. The MMP-II expression observed on GM-MØ may indicate that at least some intracellular *M. leprae* were processed. However, the processing of *M. leprae* by GM-MØ still seemed partial, since the heat-killed *M. leprae* induced T cell activation more vigorously than live bacteria, and *M. leprae*-infected DC stimulated T cells more efficiently than GM-MØ, although other factors, such as an induction of IL-12, cannot be ruled out completely. The cell wall architecture including surface-exposed molecules, of heat-killed mycobacteria is globally altered [29,30], resulting in the exudation of some soluble antigenic molecules which may be feasibly digested in macrophages (unpublished observation). Therefore, T cells are more efficiently activated by heat-killed bacteria than by live bacteria.

Table 3
Comparison of T cell-stimulating activity of live and heat-inactivated *M. leprae*[a]

M. leprae pulsed on GM-MØ (MOI)	IFN-γ (pg/ml) production by $CD4^+$ T cells after stimulation with GM-MØ at ratio (T:MØ)		
	2:1	4:1	8:1
None	2.3 ± 1.1	2.1 ± 1.2	2.4 ± 0.9
HK (40)	$406.5 \pm 49.3^{*}$	$157.3 \pm 20.1^{\ddagger}$	$75.4 \pm 6.8^{\P}$
HK (80)	$399.8 \pm 33.2^{\dagger}$	$187.7 \pm 17.8^{\S}$	$106.9 \pm 11.2^{\|}$
Live (40)	$101.5 \pm 8.8^{*}$	$30.2 \pm 4.6^{\ddagger}$	$3.2 \pm 1.9^{\P}$
Live (80)	$152.0 \pm 12.7^{\dagger}$	$82.9 \pm 7.4^{\S}$	$32.7 \pm 2.8^{\|}$

$^{*}p < 0.01$; $^{\dagger}p < 0.005$; $^{\ddagger}p < 0.005$; $^{\S}p < 0.005$; $^{\P}p < 0.005$; $^{\|}p < 0.005$.

[a] $CD4^+$ T cells (1×10^5/well) were stimulated for 4 days with autologous GM-MØ at the indicated dose of macrophage. GM-MØ were pulsed with either heat-killed (HK) or live *M. leprae* and IFN-γ (100 IU/ml) on day 3, treated with CD40L (1 μg/ml) on day 4, and were used as APC on day 5. Representatives of three separate experiments are shown. Assays were done in triplicate, and the results are expressed as the mean ± SD. Groups with identical symbols were compared using Student's *t*-test.

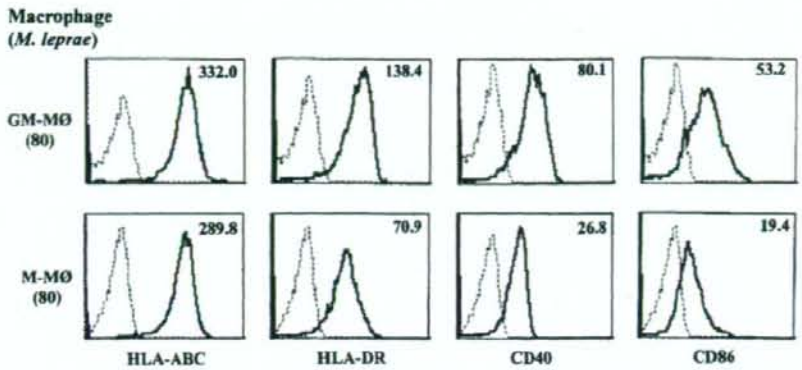

Fig. 3. Phenotype of *M. leprae*-infected GM-MØ and M-MØ. GM-MØ and M-MØ differentiated from monocytes by 3 days culture with rGM-CSF or rM-CSF were infected with *M. leprae*, treated with IFN-γ (100 IU/ml) on day 3, and further treated with CD40L (1 μg/ml) on day 4 of culture. On day 5, the phenotype of GM-MØ and M-MØ was analyzed. Dashed lines, isotype-matched control IgG; solid lines, mAb staining. The number represents the difference in mean fluorescence intensity between dashed and solid lines. Representatives of three independent experiments are shown.

Ottenhoff et al. have also reported that GM-CSF up-regulates the T cell-stimulating activity of MØ, but not M-CSF, and mycobacteria-infected GM-MØ promoted the type 1 cell-mediated immunity against pathogens [31]. Our observations are in line with their data and provide ways to enhance the cell-mediated immunity, especially in cases progressing towards lepromatous leprosy. To facilitate the T cell activation and MMP-II expression, it was required to use

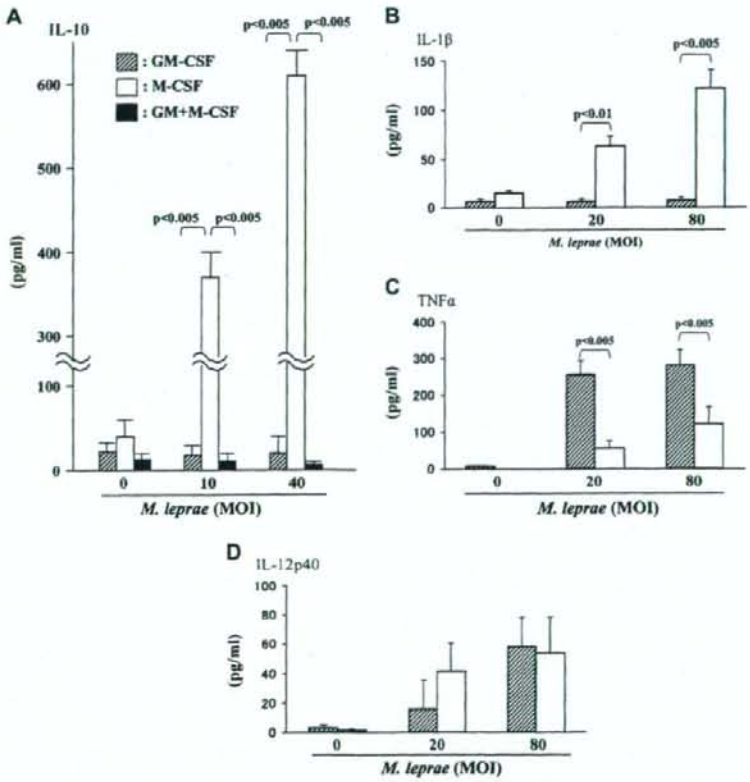

Fig. 4. Cytokine production from GM-MØ and M-MØ. MØ were differentiated by 3 days culture with rGM-CSF, rM-CSF or rGM-CSF + rM-CSF, and were stimulated with *M. leprae* for 24 h. The cytokines: (a) IL-10; (b) IL-1β; (c) TNFα; and (d) IL-12p40 were measured by ELISA. Representatives of three independent experiments are shown.

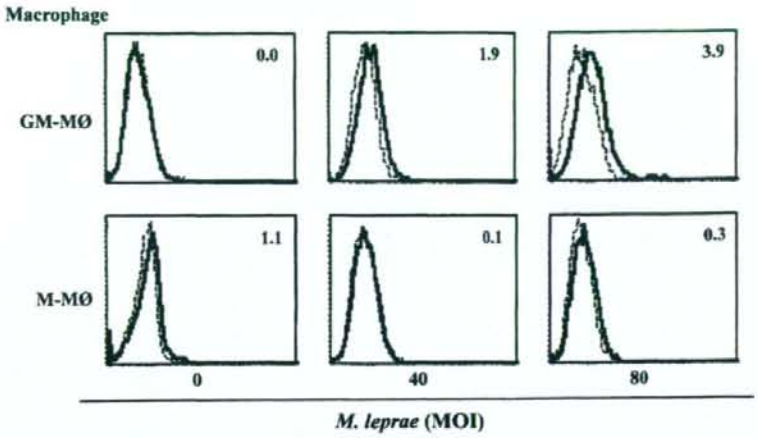

Fig. 5. Expression of MMP-II on the surface of GM-MØ and M-MØ. GM-MØ and M-MØ were differentiated from monocytes by 3 days culture with either rGM-CSF or rM-CSF, respectively. These macrophages were infected with an indicated dose of *M. leprae* and treated with IFN-γ (100 IU/ml) on day 3 of monocyte culture, further treated with CD40L (1 μg/ml) on day 4, and were analyzed for MMP-II expression on day 5. Dashed lines, control IgM; solid lines, MMP-II mAb staining. The number represents the difference in mean fluorescence intensity between dashed and solid lines. Representatives of three independent experiments are shown.

both IFN-γ and CD40L, in addition to the lineage-determining cytokine GM-CSF. IFN-γ and CD40L are probably required to compensate for the lower antigenic characteristics of *M. leprae* [24]. Studies using other mycobacteria, such as *M. bovis* BCG, may provide further useful information. Although IFN-γ is known to activate MØ for bacterial digestion and to induce IL-12p35 gene transcription [26,31], it remains to be determined if CD40L treatment on GM-MØ furthers the intracellular processing of phagosomal bacteria or whether conditioning of GM-MØ through CD40-CD40L interaction, such as in DC [32], is required for T cell stimulation. In addition to MMP-II expression, there were some differences in the phenotypic features of *M. leprae*-infected GM-MØ and M-MØ. A higher level of HLA-DR and CD86 Ags was expressed on the GM-MØ infected with *M. leprae* and co-stimulated, than on similarly treated M-MØ. The mechanism, leading to the enhanced Ag expression, especially of Ag processing by IFN-γ, has not been clearly demonstrated and remains to be elucidated, but GM-CSF, IFN-γ and CD40L seem to at least partially co-ordinate and induce the higher expression of HLA-DR and CD86. These phenotypic differences between *M. leprae*-infected GM-MØ and M-MØ again contribute to the differences in T cell stimulatory activity.

Another peculiar difference observed between the two types of MØ, GM-MØ and M-MØ, was the cytokines that they induced. IL-10 suppresses DC-dependent as well as DC-independent T cell activation [14,15,33], and creates a situation in which *M. leprae* can feasibly parasitize in the cells. While M-MØ secreted a large amount of IL-10, GM-MØ completely lacked in the production of cytokine upon stimulation with *M. leprae* (Fig. 4) or lipopolysaccharide (data not shown). Furthermore, the presence of GM-CSF diminished the IL-10 production from M-MØ by *M. leprae*. Thus, treatment of monocytes with GM-CSF can wipe off the favorable conditions for *M. leprae* survival. On the other hand, GM-MØ produced a higher level of TNFα than M-MØ. TNFα plays an important role in the granuloma formation, and TNFα is an important mediator of host defense activity in MØ, in mycobacterial lesions [34,35]. The treatment of monocyte with GM-CSF would be beneficial for MØ-mediated host defense in this respect. These observations were consistent with the previous findings that IL-10-deficient mice display increased anti-mycobacterial immunity with concordant higher levels of TNFα and a lower bacterial burden [36]. Our previous studies show that T cells from lepromatous leprosy can mount a significant production of IFN-γ by appropriate stimulation [10], therefore, the present studies may provide useful information for the development of immunotherapeutic tools, such as endogenous or exogenous treatment of macrophages with GM-CSF, and thus prevent the dissemination of *M. leprae*.

In this study, we analyzed the two types of MØ with regard to T cell-stimulating activity, and found that GM-CSF and co-stimulators enhance the host defense activity of *M. leprae*-infected MØ.

Acknowledgments

We acknowledge the contribution of Ms. N. Makino in the preparation of this manuscript. We also thank Ms. Y. Harada for technical support, and the Japanese Red Cross Society for kindly providing PBMC from healthy donors.

This work was supported in part by a Grant-in-Aid for Research on Emerging and Re-emerging Infectious Diseases and by a Grant-in-Aid for Research on HIV/AIDS from the Ministry of Health, Labour and Welfare of Japan.

References

[1] G.L. Stoner, Importance of the neural predilection of *Mycobacterium leprae* in leprosy, Lancet 2 (1979) 994–996.

[2] C.K. Job, Nerve damage in leprosy, Int. J. Lepr. Other Mycobact. Dis. 57 (1989) 532–539.
[3] S.N.C. Wemambu, J.L. Turk, M.F.R. Waters, R.J.W. Rees, *Erythema nodosum leprosum*: a clinical manifestation of the Arthus phenomenon, Lancet 2 (1969) 933–935.
[4] S. Verghese, D.G. Healey, J. Curtis, J.L. Turk, Accessory cell function of dendritic cells from lymph nodes containing *Mycobacterium leprae* induced granulomas, Int. Arch. Allergy Appl. Immunol. 87 (1988) 392–399.
[5] P. Salgame, J.S. Abrams, C. Clayberger, H. Goldstein, J. Convit, R.L. Modlin, B.R. Bloom, Differing lymphokine profiles of functional subsets of human CD4 and CD8 T cell clones, Science 254 (1991) 279–282.
[6] M. Yamamura, K. Uyemura, R.J. Deans, K. Weinberg, T.H. Rea, B.R. Bloom, R.L. Modlin, Defining protective responses to pathogens: cytokine profiles in leprosy lesions, Science 254 (1991) 277–279.
[7] P.S. Yamauchi, J.R. Bleharski, K. Uyemura, J. Kim, P.A. Sieling, A. Miller, H. Brightbill, K. Schlienger, T.H. Rea, R.L. Modlin, A role for CD40–CD40 ligand interactions in the generation of type 1 cytokine responses in human leprosy, J. Immunol. 165 (2000) 1506–1512.
[8] S.R. Krutzik, B. Tan, H. Li, M.T. Ochoa, P.T. Liu, S.E. Sharfstein, T.G. Graeber, P.A. Sieling, Y.-J. Liu, T.H. Rea, B.R. Bloom, R.L. Modlin, TLR activation triggers the rapid differentiation of monocytes into macrophages and dendritic cells, Nat. Med. 11 (2005) 653–660.
[9] Y. Maeda, T. Mukai, J. Spencer, M. Makino, Identification of an immunomodulating agent from *Mycobacterium leprae*, Infect. Immun. 73 (2005) 2744–2750.
[10] M. Makino, Y. Maeda, N. Ishii, Immunostimulatory activity of major membrane protein-II from *Mycobacterium leprae*, Cell. Immunol. 233 (2005) 53–60.
[11] D.S. Ridley, W.H. Jopling, Classification of leprosy according to immunity. A five-group system, Int. J. Lepr. Other Mycobact. Dis. 34 (1966) 255–273.
[12] D.A. Hagge, N.A. Ray, J.L. Krahenbuhl, L.B. Adams, An *in vitro* model for the lepromatous leprosy granuloma: fate of *Mycobacterium leprae* from target macrophages after interaction with normal and activated effector macrophages, J. Immunol. 172 (2004) 7771–7779.
[13] C. Frehel, N. Rastogi, *Mycobacterium leprae* surface components intervene in the early phagosome–lysosome fusion inhibition event, Infect. Immun. 55 (1987) 2916–2921.
[14] H. Jonuleit, E. Schmitt, K. Steinbrink, A.H. Enk, Dendritic cells as a tool to induce anergic and regulatory T cells, Trends Immunol. 22 (2001) 394–400.
[15] A. Granelli-Piperno, A. Golebiowska, C. Trumpfheller, F.P. Siegal, R.M. Steinman, HIV-1-infected monocyte-derived dendritic cells do not undergo maturation but can elicit IL-10 production and T cell regulation, Proc. Natl. Acad. Sci. U.S.A. 101 (2004) 7669–7674.
[16] K. Nakata, K.S. Akagawa, M. Fukayama, Y. Hayashi, M. Kadokura, T. Tokunaga, Granulocyte-macrophage colony-stimulating factor promotes the proliferation of human alveolar macrophages *in vitro*, J. Immunol. 147 (1991) 1266–1272.
[17] K.S. Akagawa, Functional heterogeneity of colony-stimulating factor-induced human monocyte-derived macrophages, Int. J. Hematol. 76 (2002) 27–34.
[18] M.U. Martin, H. Wesche, Summary and comparison of the signaling mechanisms of the Toll/interleukin-1 receptor family, Biochim. Biophys. Acta 1592 (2002) 265–280.
[19] M. Makino, M. Baba, A cryopreservation method of human peripheral blood mononuclear cells for efficient production of dendritic cells, Scand. J. Immunol. 45 (1997) 618–622.
[20] G.J. Randolph, K. Inaba, D.F. Robbiani, R.M. Steinman, W.A. Muller, Differentiation of phagocytic monocytes into lymph node dendritic cells in vivo, Immunity 11 (1999) 753–761.
[21] M. Makino, S. Shimokubo, S. Wakamatsu, S. Izumo, M. Baba, The role of human T-lymphotropic virus type 1 (HTLV-1)-infected dendritic cells in the development of HTLV-1-associated myelopathy/tropical spastic paraparesis, J. Virol. 73 (1999) 4575–4581.
[22] R.D. McDermott-Lancaster, T. Ito, K. Kohsaka, C.C. Guelpa-Lauras, J.H. Grosset, Multiplication of *Mycobacterium leprae* in the nude mouse, and some applications of nude mice to experimental leprosy, Int. J. Lepr. Other Mycobact. Dis. 55 (1987) 889–895.
[23] C.K. Stover, V.F. de la Cruz, T.R. Fuerst, J.E. Burlein, L.A. Benson, L.T. Bennett, G.P. Bansal, J.F. Young, M.H. Lee, G.F. Hatfull, S.B. Snapper, R.G. Barletta, W.R. Jacobs Jr., B.R. Bloom, New use of BCG for recombinant vaccines, Nature 351 (1991) 456–460.
[24] K. Hashimoto, Y. Maeda, H. Kimura, K. Suzuki, A. Masuda, M. Matsuoka, M. Makino, *Mycobacterium leprae* infection in monocyte-derived dendritic cells and its influence on antigen presenting function, Infect. Immun. 70 (2002) 5167–5176.
[25] S. Wakamatsu, M. Makino, C. Tei, M. Baba, Monocyte-driven activation-induced apoptotic cell death of human T-lymphotropic virus type I-infected T cells, J. Immunol. 163 (1999) 3914–3919.
[26] H. Kimura, Y. Maeda, F. Takeshita, L.E. Takaoka, M. Matsuoka, M. Makino, Upregulation of T-cell-stimulating activity of mycobacteria-infected macrophages, Scand. J. Immunol. 60 (2004) 278–286.
[27] M.M. Stefani, C.M. Martelli, T.P. Gillis, J.L. Krahenbuhl, Brazilian Leprosy Study Group, In situ type 1 cytokine gene expression and mechanisms associated with early leprosy progression, J. Infect. Dis. 188 (2003) 1024–1031.
[28] P.A. Sieling, D. Jullien, M. Dahlem, T.F. Tedder, T.H. Rea, R.L. Modlin, S.A. Porcelli, CD1 expression by dendritic cells in human leprosy lesions: correlation with effective host immunity, J. Immunol. 162 (1999) 1851–1858.
[29] P.B. Kang, A.K. Azad, J.B. Torrelles, T.M. Kaufman, A. Beharka, E. Tibesar, L.E. Desjardin, L.S. Schlesinger, The human macrophage mannose receptor directs *Mycobacterium tuberculosis* lipoarabinomannan-mediated phagosome biogenesis, J. Exp. Med. 202 (2005) 987–999.
[30] I. Vergne, J. Chua, H.H. Lee, M. Lucas, J. Belisle, V. Deretic, Mechanism of phagolysosome biogenesis block by viable *Mycobacterium tuberculosis*, Proc. Natl. Acad. Sci. U.S.A. 102 (2005) 4033–4038.
[31] F.A. Verreck, T. de Boer, D.M. Langenberg, M.A. Hoeve, M. Kramer, E. Vaisberg, R. Kastelein, A. Kolk, R. de Waal-Malefyt, T.H. Ottenhoff, Human IL-23-producing type 1 macrophages promote but IL-10-producing type 2 macrophages subvert immunity to (myco)bacteria, Proc. Natl. Acad. Sci. U.S.A. 101 (2004) 4560–4565.
[32] C. Caux, C. Massacrier, B. Vanbervliet, B. Dubois, C. Van Kooten, I. Durand, J. Banchereau, Activation of human dendritic cells through CD40 cross-linking, J. Exp. Med. 180 (1994) 1263–1272.
[33] K. Mochida-Nishimura, K.S. Akagawa, E.A. Rich, Interleukin-10 contributes development of macrophage suppressor activities by macrophage colony-stimulating factor, but not by granulocyte-macrophage colony-stimulating factor, Cell. Immunol. 214 (2001) 81–88.
[34] J.H. Davis, H. Clay, J.L. Lewis, N. Ghori, P. Herbomel, L. Ramakrishnan, Real-time visualization of mycobacterium–macrophage interactions leading to initiation of granuloma formation in zebrafish embryos, Immunity 17 (2002) 693–702.
[35] E. Giacomini, E. Iona, L. Ferroni, M. Miettinen, L. Fattorini, G. Orefici, I. Julkunen, E.M. Coccia, Infection of human macrophages and dendritic cells with *Mycobacterium tuberculosis* induces a differential cytokine gene expression that modulates T cell response, J. Immunol. 166 (2001) 7033–7041.
[36] P.J. Murray, R.A. Young, Increased antimycobacterial immunity in interleukin-10-deficient mice, Infect. Immun. 67 (1999) 3087–3095.

JOURNAL OF BACTERIOLOGY, Jan. 2006, p. 86–95
0021-9193/06/$08.00+0 doi:10.1128/JB.188.1.86–95.2006

Vol. 188, No. 1

Identification and Characterization of the Genes Involved in Glycosylation Pathways of Mycobacterial Glycopeptidolipid Biosynthesis

Yuji Miyamoto,[1] Tetsu Mukai,[1] Noboru Nakata,[1] Yumi Maeda,[1] Masanori Kai,[1] Takashi Naka,[2] Ikuya Yano,[2] and Masahiko Makino[1]*

Department of Microbiology, Leprosy Research Center, National Institute of Infectious Diseases, 4-2-1 Aobacho, Higashimurayama, Tokyo 189-0002, Japan,[1] and Japan BCG Central Laboratory, 3-1-5 Matsuyama, Kiyose, Tokyo 204-0022, Japan[2]

Received 2 August 2005/Accepted 10 October 2005

Glycopeptidolipids (GPLs) are major components present on the outer layers of the cell walls of several nontuberculous mycobacteria. GPLs are antigenic molecules and have variant oligosaccharides in mycobacteria such as *Mycobacterium avium*. In this study, we identified four genes (*gtf1*, *gtf2*, *gtf3*, and *gtf4*) in the genome of *Mycobacterium smegmatis*. These genes were independently inactivated by homologous recombination in *M. smegmatis*, and the structures of GPLs from each gene disruptant were analyzed. Thin-layer chromatography, gas chromatography–mass spectrometry, and matrix-assisted laser desorption ionization–time-of-flight mass spectrometry analyses revealed that the mutants Δgtf1 and Δgtf2 accumulated the fatty acyl-tetrapeptide core having *O*-methyl-rhamnose and 6-deoxy-talose as sugar residues, respectively. The mutant Δgtf4 possessed the same GPLs as the wild type, whereas the mutant Δgtf3 lacked two minor GPLs, consisting of 3-*O*-methyl-rhamnose attached to *O*-methyl-rhamnose of the fatty acyl-tetrapeptide core. These results indicate that the *gtf1* and *gtf2* genes are responsible for the early glycosylation steps of GPL biosynthesis and the *gtf3* gene is involved in transferring a rhamnose residue not to 6-deoxy-talose but to an *O*-methyl-rhamnose residue. Moreover, a complementation experiment showed that *M. avium gtfA* and *gtfB*, which are deduced glycosyltransferase genes of GPL biosynthesis, restore complete GPL production in the mutants Δgtf1 and Δgtf2, respectively. Our findings propose that both *M. smegmatis* and *M. avium* have the common glycosylation pathway in the early steps of GPL biosynthesis but differ at the later stages.

The mycobacterial cell envelope has a unique structure that contains a complex of covalently linked peptidoglycan, arabinogalactan, and mycolic acids (7, 11). The outer layer of the cell envelope is composed of several types of glycolipids that affect the surface properties of mycobacterial cells (7, 11). Glycopeptidolipids (GPLs) are a major class of glycolipid present on the outer layer of several species of nontuberculous mycobacteria, such as *Mycobacterium avium* complex, *M. scrofulaceum*, *M. chelonae*, *M. fortuitum*, and *M. smegmatis* (31). GPLs have a common fatty acyl-tetrapeptide core consisting of tetrapeptide amino alcohol (D-Phe-D-*allo*-Thr-D-Ala-L-alaninol) and amide-linked long-chain fatty acid (C_{26-34}). The fatty acyl-tetrapeptide core is glycosylated with 6-deoxy-talose (6-d-Tal) and variable *O*-methyl-rhamnose (*O*-Me-Rha) residues, termed non-serovar-specific GPLs (nsGPLs), which are also the main products of *M. smegmatis* GPLs (1, 4, 10). The GPLs of *M. avium* have a more complicated structure, in which an additional Rha residue is added to 6-d-Tal of nsGPLs to be extended with various haptenic oligosaccharides, which are important surface antigens, resulting in serovar-specific GPLs (ssGPLs) (1, 4, 31).

There are some evidences that GPLs may be responsible for pathogenicity. It has been shown that the some of the ssGPLs are immunosuppressive and are able to induce a variety of cytokines, which affect host responses to infection (3, 15, 18, 29). Also, ssGPLs are identified as the factors modulating the phagocytosis and phagosome-lysosome fusion (17, 21). The altered GPL structure is also known to affect the colony morphology relevant to variable virulence (14, 30).

The biosyntheses of GPLs, particularly nsGPLs, have been characterized for *M. smegmatis*. Several biosynthetic genes encoding enzymes such as *O*-methyltransferase, acetyltransferase, and peptide synthetase have been identified (5, 16, 25, 26), but less is known about the genes involved in the glycosylation steps of the GPLs. The only glycosyltransferase gene that has been characterized is *rtfA* from *M. avium*, which is responsible for transferring the Rha residue to 6-d-Tal of nsGPLs to form ssGPLs (12). However, the initial glycosylation steps for the formation of nsGPLs remain unknown. Recently, it was shown that GPLs from *M. smegmatis* has a unique structure in which nsGPLs are further glycosylated, unlike ssGPLs (23, 24, 32), but these unique GPLs are produced in a carbon-starved situation, which is not a normal growth condition.

In this study, to clarify the glycosylation step leading to the formation of nsGPLs and its further products, we focused on four of the *M. smegmatis* genes having high similarity to *M. avium rtfA*, whose functions remain uncharacterized. Here, we have undertaken the gene disruption approach for generating each mutant in *M. smegmatis*, characterized their biochemical phenotypes, and finally hypothesized new biosynthetic pathways associated with glycosylation of GPLs.

* Corresponding author. Mailing address: Department of Microbiology, Leprosy Research Center, National Institute of Infectious Diseases, 4-2-1 Aobacho, Higashimurayama, Tokyo 189-0002, Japan. Phone: 81-42-391-8059. Fax: 81-42-391-8212. E-mail: mmaki@nih.go.jp.

TABLE 1. Bacterial strains and vectors used in this study

Strain or vector	Characteristic(s)	Source or reference
Bacteria		
E. coli		
DH5α	Cloning host	
STBL2	Cloning host	
M. smegmatis		
mc^2155	Wild type	27
Δgtf1	*gtf1* disruptant	This study
Δgtf2	*gtf2* disruptant	This study
Δgtf3	*gtf3* disruptant	This study
Δgtf4	*gtf4* disruptant	This study
M. avium		
JATA51-01 (ATCC 25291)	Source of *gtfA* and *gtfB*	
Vectors		
pYUB854	Cosmid vector	2
phAE87	Phasmid vector carrying full-length DNA of mycobacteriophage PH101	2
pMV261	*E. coli-Mycobacterium* shuttle vector carrying *hsp60* promoter cassette	28
pYUBgtf1	pYUB854 with *gtf1*-disrupted sequences for generating recombinant mycobacteriophage	This study
pYUBgtf2	pYUB854 with *gtf2*-disrupted sequences for generating recombinant mycobacteriophage	This study
pYUBgtf3	pYUB854 with *gtf3*-disrupted sequences for generating recombinant mycobacteriophage	This study
pYUBgtf4	pYUB854 with *gtf4*-disrupted sequences for generating recombinant mycobacteriophage	This study
pMVgtf1	pMV261 with *gtf1*	This study
pMVgtf2	pMV261 with *gtf2*	This study
pMVgtf3	pMV261 with *gtf3*	This study
pMVgtf4	pMV261 with *gtf4*	This study
pMVgtfA	pMV261 with *gtfA*	This study
pMVgtfB	pMV261 with *gtfB*	This study

MATERIALS AND METHODS

Bacterial strains, culture conditions, and DNA manipulation. Bacterial strains and vectors used and constructed are listed in Table 1. Mycobacterial strains for DNA manipulation were grown in Middlebrook 7H9 broth (Difco) with 0.05% Tween 80 or Middlebrook 7H10 agar (Difco) with 0.5% glycerol, and each was supplemented with 10% albumin-dextrose-catalase enrichment (Difco). *M. smegmatis* strains for GPL production were cultured in Luria-Bertani (LB) broth with 0.05% Tween 80. DNA manipulation including isolation of DNA, transformation, and PCR was carried out as described previously (22). *E. coli* strain DH5α was used for routine manipulation and propagation of plasmid DNA. *E. coli* strain STBL2 was used for construction of phasmid vectors derived from phAE87. Antibiotics was added as required: kanamycin, 50 μg/ml for *E. coli* and 25 μg/ml for *M. smegmatis*; hygromycin B, 150 μg/ml for *E. coli* and 75 μg/ml for *M. smegmatis*.

Generation of the gene disruptants. The targeted genes (*gtf1*, *gtf2*, *gtf3*, and *gtf4*) were selected by BLAST analysis of unfinished *M. smegmatis* genome sequences deposited in the database of The Institute for Genomic Research (TIGR) (http://www.tigr.org) with the *rtfA* gene of *M. avium* as the query nucleotide sequence. Each gene was inactivated by inserting a hygromycin-resistant cassette (*hyg*) using the specialized transducing phage system (2). To construct the disrupted sequences, around 1.0-kb fragments both upstream and downstream of each gene were amplified from *M. smegmatis* mc^2155 genomic DNA using the following two pairs of primers: US1 and UA1 for upstream of *gtf1* and DS1 and DA1 for downstream of *gtf1*; US2 and UA2 for upstream of *gtf2* and DS2 and DA2 for downstream of *gtf2*; US3 and UA3 for upstream of *gtf3* and DS3 and DA3 for downstream of *gtf3*; US4 and UA4 for upstream of *gtf4* and DS4 and DA4 for downstream of *gtf4*. The PCR products were digested with each restriction enzyme and cloned into the corresponding sites flanking *hyg* of pYUB854 to give pYUBgtf1 (*gtf1*), pYUBgtf1 (*gtf2*), pYUBgtf3 (*gtf3*), and pYUBgtf4 (*gtf4*). These plasmids were used for packaging into the phasmid vector phAE87 to construct a specialized transducing mycobacteriophage for gene disruption as described previously (2). The *M. smegmatis* mc^2155 strain infected with the above mycobacteriophage at a multiplicity of infection of 10 was incubated at 37°C for 3 h in 7H9 broth without Tween 80. Harvested bacterial cells were then plated and cultured on 7H10 agar containing 75 μg/ml hygromycin B for 1 week. The hygromycin B-resistant colonies were selected, and their genomic DNA was subjected to PCR analysis to confirm the disruption of each gene using the following primers: U1 and D1 for *gtf1*; U2 and D2 for *gtf2*; U3 and D3 for *gtf3*; and U4 and D4 for *gtf4* (Fig. 1A to D).

Construction of the *gtf* expression vectors. The *gtf* genes of *M. smegmatis* and *M. avium* were amplified from each genomic DNA using the following primers: GTF1S and GTF1A for *gtf1*, GTF2S and GTF2A for *gtf2*, GTF3S and GTF3A for *gtf3*, GTF4S and GTF4A for *gtf4*, GTFAS and GTFAA for *gtfA*, and GTFBS and GTFBA for *gtfB*. The PCR products were digested with each restriction enzyme and cloned into the corresponding site of pMV261 to give pMVgtf1 (for the *gtf1* gene), pMVgtf2 (for the *gtf2* gene), pMVgtf3 (for the *gtf3* gene), pMVgtf4 (for the *gtf4* gene), pMVgtfA (for the *gtfA* gene), and pMVgtfB (for the *gtfB* gene). These vectors were used for complementation and overexpression experiment.

Isolation and purification of GPLs. The total lipids were extracted from harvested bacterial cells with $CHCl_3/CH_3OH$ (2:1, vol/vol) for several hours at room temperature. The extracts from the organic phase were separated from the aqueous phase and evaporated to dryness. For isolation of crude deacylated GPLs, total lipid fractions were subjected to mild alkaline hydrolysis as previously described (22, 25). For analytical thin-layer chromatography (TLC), the total lipid fraction after mild alkaline hydrolysis was spotted on silica gel 60 plates (Merck) and developed in $CHCl_3$-CH_3OH (9:1 [vol/vol]). Deacylated GPLs and other compounds were visualized by spraying with 10% H_2SO_4 and charring. Each total lipid fraction was extracted from an equal weight of harvested cells. Purified deacylated GPLs were separated from the total lipid fraction after mild alkaline hydrolysis by preparative TLC on the same plates and extracted from the bands corresponding to each GPLs. β-Elimination and perdeuteriomethylation treatment for determination of the linkage positions of sugar moieties were carried out as described previously (6, 9, 12).

GC/MS analysis. For monosaccharide analysis, purified deacylated GPLs or total lipid fraction after mild alkaline hydrolysis was hydrolyzed in 2 M trifluoroacetic acid (2 h, 120°C), and released sugars from deacylated GPLs were reduced with $NaBD_4$ (sodium borodeuteride) and then acetylated with pyridine-acetic anhydride (1:1 [vol/vol]) at room temperature overnight. Each total lipid fraction was extracted from an equal weight of harvested cells. The resulting

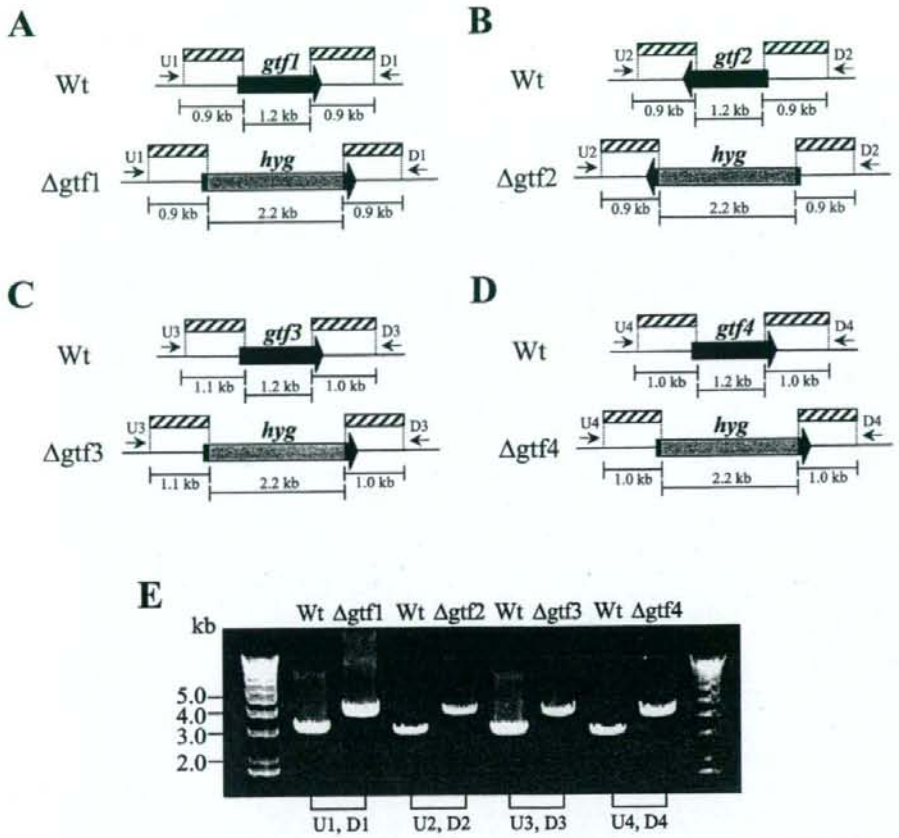

FIG. 1. Generation of *gtf* gene disruptants. (A to D) Schematic diagram of each *gtf* region on the chromosome of the wild-type *M. smegmatis* mc^{2}155 strain (Wt) and its gene disruptants Δgtf1, Δgtf2, Δgtf3, and Δgtf4. The shaded boxes indicate the regions included in recombinant phage for gene disruption. The black arrows represent the coding region of each *gtf* gene. The gray boxes represent the hygromycin resistance cassette (*hyg*). The primers used for PCR analysis are indicated by small arrows. (E) PCR analyses of the wild type and each disruptant using the primers indicated above.

alditol acetates were separated and analyzed by gas chromatography–mass spectrometry (GC/MS) on TRACE DSQ (Thermo electron) instrument equipped with an SP-2380 column (SUPELCO) using helium gas. The temperature program was from 52 to 172°C at 40°C/min and then 172 to 250°C at 3°C/min.

MALDI-TOF/MS analysis. To determine the total mass of the purified deacylated GPLs, matrix-assisted laser desorption ionization–time-of-flight (MALDI-TOF) mass spectra (in the positive mode) were acquired on a QSTAR XL (Applied Biosystems) with a pulse laser emitting at 337 nm. Samples mixed with 2,5-dihydroxybenzoic acid as the matrix were analyzed in the reflectron mode with an accelerating voltage operating in positive ion mode of 20 kV.

RESULTS

Disruption of *gtf1*, *gtf2*, *gtf3*, and *gtf4* by allelic exchange. Four genes showing high similarity to the *rtfA* gene, involved in GPL biosynthesis of *M. avium*, were identified for the *M. smegmatis* mc^{2}155 strain (12). The homologies of their corresponding amino acid sequences with that of RtfA were around 60%. Three genes were found in the GPL biosynthetic gene cluster, namely, *gtf1*, *gtf2*, and *gtf3* (GenBank accession no. AY138899.1) (16), whereas one gene, designated *gtf4* (TIGR database no. 4839918 to 4841162), was located far from the other three genes. To examine whether these genes are responsible for GPL biosynthesis, we generated four gene disruptants, designated Δgtf1, Δgtf2, Δgtf3, and Δgtf4, using the specialized transducing mycobacteriophage containing the entire open reading frame, replacing with the hygromycin resistance cassette (2). For confirmation of the gene disruption, PCR analysis was performed on chromosomal DNA from each disruptant. To avoid the amplification of disrupted sequences derived from residual mycobacteriophage, we designed and used the primers located outside the sequences included in each mycobacteriophage as shown in Fig. 1A to D. As expected, around 3.0-kb fragments were amplified from mc^{2}155 (wild type), whereas around 4.0-kb fragments were amplified from each disruptant, because most of the *gtf* coding region (1.2 kb) was replaced by the hygromycin resistance cassette (2.2 kb) (Fig. 1E). These results demonstrated that allelic exchanges involving replacement of the *gtf* genes with the disrupted constructs have been successful.

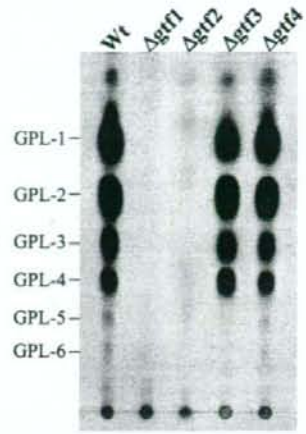

FIG. 2. TLC analyses of crude GPL extracts from the *M. smegmatis* mc^2155 strain (Wt) and its gene disruptants. The total lipid fraction after mild alkaline hydrolysis was spotted on plates and developed in $CHCl_3$-CH_3OH (9:1 [vol/vol]). GPLs were visualized by spraying with 10% H_2SO_4 and charring. Each total lipid fraction was extracted from an equal weight of harvested cells.

TLC analysis of gene disruptants. To investigate the effects of the mutation in each *gtf* gene, we examined GPL production of four gene disruptants. TLC analyses of total lipid fraction after mild alkaline hydrolysis revealed that wild-type mc^2155 mainly produced six components, designated GPL-1 to -6, whereas Δgtf1 and Δgtf2 lacked all six components and Δgtf3 lacked two minor ones (GPL-5 and GPL-6) found in the wild type (Fig. 2). In contrast, no differences in TLC profile were observed between Δgtf4 and the wild type (Fig. 2).

Characterization of Δgtf1 and Δgtf2. In Δgtf1 and Δgtf2, the TLC analyses showed that six GPL components contained in the wild type had disappeared. On the other hand, there is the possibility that both disruptants contained GPL derivatives which are structurally incomplete and hard to be detected by TLC analyses. To characterize the sugars included in GPL derivatives from both disruptants and to compare with the wild type, each total lipid fraction after mild alkaline hydrolysis was hydrolyzed, and the released monosaccharides as their alditol acetates were examined by GC/MS. Figure 3 shows that the profiles of the wild type gave three peaks corresponding to 2,3,4-tri-*O*-Me-Rha, 3,4-di-*O*-Me-Rha, and 6-d-Tal (Fig. 3A), whereas Δgtf1 lacked 6-d-Tal (Fig. 3B) and Δgtf2 lacked 3,4-di-*O*-Me-Rha and 2,3,4-tri-*O*-Me-Rha (Fig. 3C). Complementation of both disruptants with each respective gene restored the TLC profile of GPLs to that observed for the wild type (not shown). Therefore, the *gtf1* and *gtf2* genes are found to be responsible for transferring the 6-d-Tal and Rha residues, respectively.

Structural determination of GPL-5 and GPL-6 for characterization of Δgtf3. The TLC profile of Δgtf3 showed that two spots (GPL-5 and GPL-6) disappeared (Fig. 2). To reveal the biosynthetic role of the *gtf3* gene, GPL-5 and GPL-6 were purified from mc^2155 and their structures were determined. GC/MS analyses showed that GPL-5 and GPL-6 contained 6-d-Tal and 3,4-di-*O*-Me-Rha, which were identified as sugar

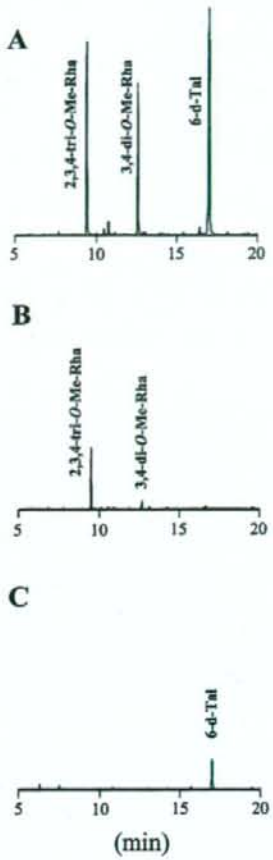

FIG. 3. GC/MS analyses of alditol acetates of sugars released from crude GPLs. GPLs were extracted from *M. smegmatis* strains: (A) mc^2155 strain, (B) Δgtf1, and (C) Δgtf2. Alditol acetate derivatives were prepared from the total lipid fraction after mild alkaline hydrolysis, which was extracted from an equal weight of harvested cells.

moieties of GPL-3 and GPL-4 (Fig. 4A). However, an extra sugar, 3-*O*-Me-Rha, was also detected (Fig. 4A). MALDI-TOF/MS analyses revealed that the main molecular ions of GPL-5 (*m/z* 1,333.8) and GPL-6 (*m/z* 1,319.8) were 160 mass units higher than those of GPL-3 (*m/z* 1,173.9) and GPL-4 (*m/z* 1,159.9), respectively (Fig. 4B). These results confirmed the presence of 3-*O*-Me-Rha in GPL-5 and GPL-6 and also suggested that 3-*O*-Me-Rha was further added to GPL-3 and GPL-4. Although GPL-5 and GPL-6 contained same three sugars, the spectra showed that the main molecular ion of GPL-5 (*m/z* 1,333.8) was 14 mass units higher than that of GPL-6 (*m/z* 1,319.8) (Fig. 4Ba and 4Bb). These differences in total mass may be due to O methylation of fatty acid as observed in structures of GPL-1 and GPL-3, suggesting that fatty acid of GPL-5 was O methylated like GPL-1 and GPL-3 (16). To investigate the sugar linked to D-*allo*-Thr of the fatty acyltetrapeptide core, GPL-5 and GPL-6 were subjected to β-elimination treatment. The main ion peaks of treated GPL-5 and

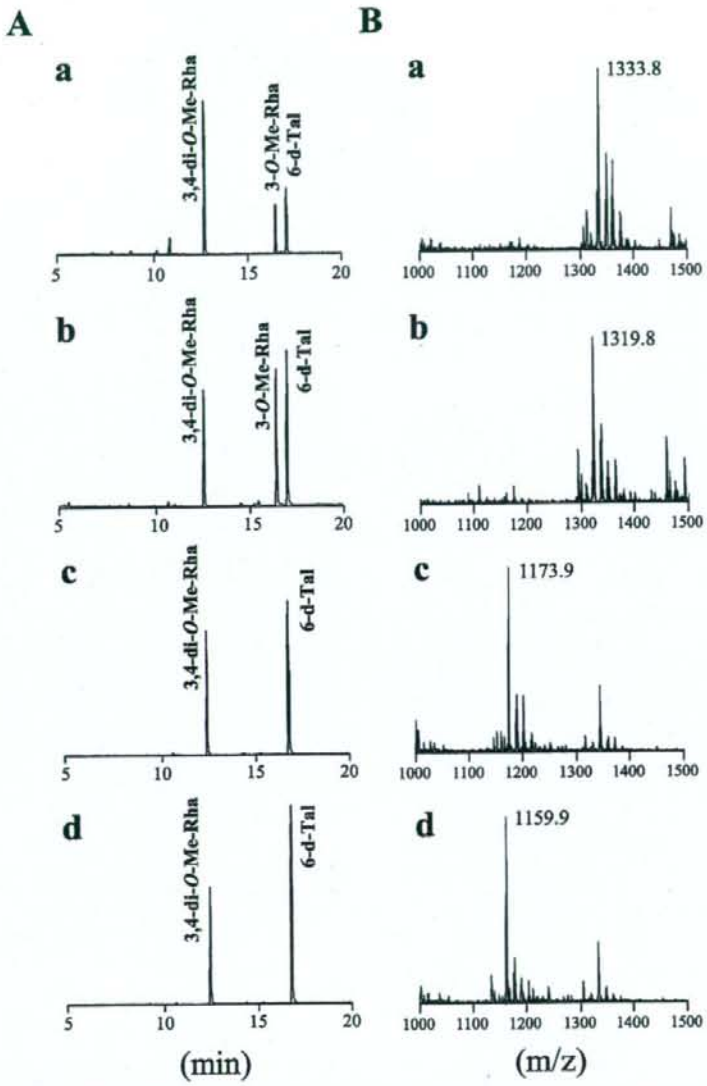

FIG. 4. Biochemical characterization of GPL-5 (a), GPL-6 (b), GPL-3 (c), and GPL-4 (d). (A) GC/MS analysis of alditol acetates of sugars released from each purified GPL. (B) MALDI-TOF/MS analysis of total molecular mass of each purified GPLs. (C) MALDI-TOF/MS analysis of total molecular mass of purified GPL-5 (a) and GPL-6 (b), which were subjected to β-elimination.

GPL-6 were *m/z* 1,171.7 and 1,157.7, respectively, which resulted in the loss of total mass of 162, suggesting that 6-d-Tal was linked to the position of D-*allo*-Thr (Fig. 4C). The linkage position of the sugars linked to the L-alaninol site of GPL-5 and GPL-6 was then determined by GC/MS analyses followed by perdeuteriomethylation. As shown in Fig. 5A, the GC profiles of alditol acetates from perdeuteriomethylated GPL-5 gave three peaks corresponding to 6-d-Tal, 3-*O*-Me-Rha, and 3,4-di-*O*-Me-Rha. The characteristic spectra of 3-*O*-Me-Rha and 3,4-di-*O*-Me-Rha, which are predicted to be linked to L-alaninol, are illustrated in Fig. 5B and C, respectively. The spectrum of 3-*O*-Me-Rha gave fragment ions at *m/z* 121, 134, and 165, which represent the presence of a deuteriomethyl group at positions C-2 and C-4. In contrast, no deuteriomethyl group was observed in 3,4-di-*O*-Me-Rha, whose C-2 position was acetylated, supported by the detection of fragment ions at *m/z* 131 and 190. The results from GC/MS analyses of perdeuteriomethylated GPL-6 were the same as those for GPL-5 (not shown). These observations demonstrated that GPL-5 and GPL-6 have the same sugar moieties, which are 6-d-Tal at